PREDICTION OF UNSTEADY AERODYNAMIC LOADS AND WAKE STRUCTURE OF WIND TURBINE IN YAWED INFLOW

Hakjin Lee, hakjin@kaist.ac.kr, Korea Advanced Institute of Science and Technology (Republic of Korea)

Duck-Joo Lee, djlee2@kaist.ac.kr, Korea Advanced Institute of Science and Technology (Republic of Korea)

Abstract

A wind turbine is becoming as one of the most promising and cost-effective renewable energy sources, due to its economic merits and technical maturity. It especially spends considerable time under yawed flow condition during operating time. Under the yawed flow condition, a velocity component parallel to the rotating plane exists, and this leads to skewed wake structures. Because of the skewed wake geometry, the trailing and shed wake vortices unequally expand, and asymmetric inflow distribution on the rotor blades, a strong wake-wake interaction between the hub and tip vortices, and the curled vorticity fields around the rotor area occur. Consequently, the yawing angle causes an azimuthal variation in the aerodynamic loads, thus leading to structural damage to wind turbine components. In the present study, the impacts of the skewed wake on the aerodynamic performance of a wind turbine were numerically investigated and discussed in detail. For this purpose, the nonlinear vortex lattice method coupling with a time-accurate vortex particle method was used. A numerical simulation of the TU Delft and NREL Phase VI wind turbine models was carried out, and predicted results were compared against measurements. The results showed that the aerodynamic loads can be accurately calculated, even for highly yawed flow conditions and complex wake dynamics can be clearly observed.

1. INTRODUCTION

Wind turbines are subjected to various unsteady and transient environment conditions such as yaw misalignment, atmospheric turbulence, wind shear flow, and gusts. They spend a considerable time under the yawed flow condition that the wind direction is not parallel to the rotating axis of wind turbine. When yaw misalignment is present, the rotor blades experience an unsteady aerodynamic behaviour with radial and azimuthal position. This may have a negative impact on the fatigue lifetime of the rotor blades and cause structural damage to wind turbine's components as well as reduction in the quality of power generation.

The cycle-to-cycle variation in aerodynamic loads are mainly attributed to the skewed wake effect at low wind speeds, since the complicated vortex structures in the skewed wake are responsible for the asymmetrical distribution of induced velocity on the rotor plane. Therefore, a study on the propagation of the skewed wake and its unsteady characteristics is becoming more prominent in the area of wind turbines. However, it still remains a challenging problem because of the complexity of the skewed wake structure.

The aerodynamic performance and time-varying blade loading of wind turbines under yawed flow conditions were evaluated and compared against the experimental results using various numerical methods by Ryu et al. (Ref. 1), Dueque et al. (Ref. 2), Shen et al. (Ref. 3), Tongchitpakdee et al. (Ref. 4), and Yu et al. (Ref. 5). However, many studies have focused mainly on predicting the aerodynamic performance of yawed wind turbines, hence they have tried to yield more accurate aerodynamic loads acting on the rotor blades without sufficient consideration of wake characteristics.

The measurements on a small-scale wind turbine performance and wake geometries with various operating conditions including tip speed ratio, tip pitch angle, and yaw angles, were carried out by Vermmer (Refs. 6, 7) and Haans et al. (Refs. 8, 9). Experimental studies on the skewed wake using optimal equipment were conducted to measure the tip vortex trajectories and wake deflection by Grant et al. (Ref. 10) and Grant and Parkin (Ref. 11). Using the flow visualization method, the wake flow behind the yawed rotor model was measured to investigate the effect of incoming atmospheric boundary-layer (ABL) and the turbulent inflow conditions on the wake characteristics by Bastankhah and Porté-Agel (Ref. 12), and Bartl and Sætran (Ref. 13), respectively. Howland et al. (Ref. 14) observed the curled wake morphology and discussed the transient wake behaviours in detail.

The main objective of the present study is to numerically predict the aerodynamic loads acting on the rotor blades under yawed flow conditions. In addition, the effects of skewed wake structures on the aerodynamic characteristics are discussed in detail. In this works, the numerical simulation on the TU Delft and NREL Phase VI wind turbine model, exposed to a low wind speed with different

Presented at 44th European Rotorcraft Forum, Delft, The Netherlands, 19-20 September, 2018

yaw angles, was carried out. For these purposes, nonlinear vortex lattice method (NVLM) is used for predicting loads and vortex particle method (VPM) is adopted to model the shedding rotor wake. The aerodynamic and wake models used in this study are validated by comparing results against the measurements on TU Delft rotor. Current works can help to achieve a better understanding of the wake-induced phenomena and evolving pattern of the deflected wake.

2. METHODOLOGY

2.1. Nonlinear vortex lattice method

Vortex methods would be a better approach to analyse the wind turbine aerodynamics and wake dynamics since the rotor blades of wind turbine mostly experience the incompressible flow. In addition, they can preserve the wake structures in the downstream without the numerical dissipation error. In the present work, nonlinear vortex lattice method (NVLM) is used to predict the unsteady aerodynamic loads acting on the rotor blades, and study the impact of a skewed wake geometry in yawed rotor configuration. Aforementioned, NVLM has been suggested to overcome the inherent drawbacks of the classical vortex lattice method (VLM) that is not able to consider the nonlinear aerodynamic characteristics occurring on low-Reynolds number flow or stalled flow at the high angle of attack. This can be possible by applying the airfoil look-up table at a control point and iterative vortex strength correction to the VLM. The inflow velocity and effective angle of attack at the control points should be evaluated, as shown in Eq. (1) and (2) respectively. The most suitable location of the control points was determined as a half chord of camber line from the previous studies, and a detailed description of derivations is out of scope for this paper, and is discussed in the references (Refs. 15, 16).

(1) $$\mathbf{V}_{\text{inflow}} = \mathbf{V}_{\infty} - \mathbf{\Omega} \times \mathbf{r} + \mathbf{V}_{\text{ind,bound}} + \mathbf{V}_{\text{ind,wake}}$$

(2) $$\alpha_{\text{eff}} = \alpha_{\text{inflow}} - \phi_{geo} = \tan^{-1}\left(\frac{\mathbf{V}_{\text{inflow}} \cdot \mathbf{a}_3}{\mathbf{V}_{\text{inflow}} \cdot \mathbf{a}_1}\right) - \phi_{geo}$$

where $\mathbf{V}_{\text{inflow}}$ is the inflow velocity, $\mathbf{V}_{\infty}$ is the free stream velocity, $\mathbf{\Omega} \times \mathbf{r}$ is the rotational velocity, $\mathbf{V}_{\text{ind,bound}}$ is the self-induced velocity, and $\mathbf{V}_{\text{ind,wake}}$ is the wake-induced velocity, respectively. α_{eff} is the effective angel of attack, α_{inflow} is the local inflow angle and ϕ_{geo} is the local geometric pitch angle including twist angle and collective pitch angle each blade section in the radial direction. $\mathbf{a}_1$ and $\mathbf{a}_3$ are the unit vectors along the tangential and normal to the rotating plane.

NVLM is also incorporated in a vortex particle method (VPM) for modelling the wind turbine wake shed from trailing edge of blades. A detailed description for wake model is discussed in the following section.

2.2. Vortex particle method

The understanding and accurate prediction of the wind turbine wake are important because the wake structure is critical in the estimation of the wind turbine performance. In the present study, the vortex particle method (VPM) developed for rotor flow simulation was employed to model the wind turbine wake. (Ref. 17) The rotor wake shed from the trailing edge of a full span of rotor blades were represented as a number of vortex particles instead of vortex filaments. The vortex particles can be regarded as concentrated vortices within a certain volume, namely a small section of a vortex tube. The strength of the recently shed vortex particles was already determined at the previous time step by imposing Kutta condition at the vortex elements placed at the trailing edge. These particles mutually affect each other and is allowed to freely distort and move to the downstream. Therefore, their location and convection velocity should be updated during time-marching steps. The convection velocity is the sum of the free stream velocity, the self-induced velocity due to the bound vortices, and the wake-induced velocity due to wake vortices. The velocity induced by the wake particles is calculated using the Biot–Savart law and high-order algebraic smoothing function (Ref. 18), and second-order Runge–Kutta method was used for the numerical time integration (Ref. 19, 20).

The vorticity field can be represented by a set of *S* number of Lagrangian vector-valued particles as shown in Eq. (3) and (4).

(3) $$\boldsymbol{\omega}(\mathbf{x},t) = \sum_{i=1}^{S} \boldsymbol{\alpha}_i(t)\zeta_\sigma\left(\mathbf{x} - \mathbf{x}_i(t)\right)$$

$$\boldsymbol{\omega}(\mathbf{x},t) = \sum_{i=1}^{S} V_i \boldsymbol{\omega}_i(\mathbf{x}_i,t)\zeta_\sigma\left(\mathbf{x} - \mathbf{x}_i(t)\right)$$

(4) $$\zeta_\sigma(\mathbf{r}) = \frac{1}{\sigma_3}\frac{15}{8\pi}\left[\left(\frac{|\mathbf{r}|}{\sigma}\right)^2 + 1\right]^{-7/2}$$

where $\boldsymbol{\omega}(\mathbf{x},\mathrm{t})$ is the vorticity in the wake, $\boldsymbol{\alpha}_i(t)$ is a strength vector, and V_i is the volume of *i*-th vortex particle. $\mathbf{x}$ is the position vector of an arbitrary point in the field, $\mathbf{x}_i$ is the position vector of *i*-th vortex particle, and $\mathbf{r}$ is the distance between $\mathbf{x}$

Presented at 44th European Rotorcraft Forum, Delft, The Netherlands, 19-20 September, 2018

and $\mathbf{x}_i$, Furthermore, σ is a smoothing radius and $\zeta_\sigma(\rho)$ is the three-dimensional regularization function or smoothing function which is needed to avoid a singularity problem.

A large number of vortex particles were generated during the time-marching step for wake evolution. The computing time for evaluating the convection velocity of each vortex particle considerably increases as the number of vortex particles in the downstream increases. Therefore, a capability of multicore processor technology was employed to calculate the induced velocities at each vortex particle. The increasing availability and capability of high-performance computing can help alleviate the computational burden.

2.3. Blade and wake modeling

For NVLM simulation, the wind turbine blade is modelled by a number of vortex elements placed on the camber surface. In this current work, the blades of TU Delft and NREL Phase VI rotor models were discretized by using 20 (chordwise) × 40 (spanwise) quadrilateral vortex ring elements with a grid clustering near inboard and outboard locations. The simulation was conducted for a total 20 revolutions including 1 revolution of slowly starting rotation to prevent a numerical instability problem occurring in the wake solution caused by an impulsive rotation. When the wind turbine was exposed to yawed inflow condition, this will cause the unsteady variation in the aerodynamic loads and the formation of skewed wake. Hence, the step size for the time marching should be small enough to ensure that the unsteady aerodynamic behaviour and complex wake evolution can be captured. A discretization of the time step $\Delta\psi = 5°$ was used here.

3. RESULTS AND DISCUSSION

3.1. TU Delft rotor model

3.1.1. Model description

A notable experiment campaign was carried out in an open jet tunnel at the Delft University of Technology (DUT) to investigate the wind turbine aerodynamics and near wake aerodynamics of a small-scale wind turbine. Vermeer et al. (Refs. 6, 7) conducted the experiments with a two-bladed wind turbine model to measure both axial forces acting on the rotor blades and tip vortex locations in the axial flow conditions. The rotor thrust forces normal to the rotating plane were recorded by the strain gauges and wake geometries behind the rotor blade were captured by the flow visualization technique. The subsequent experiment has been performed by Haans et al. (Ref. 8, 9) and it was a follow up of the first experiments with similar wind turbine configuration and flow conditions. A detailed description of the rotor model is listed in Table 1.

Table 1. Model description of TU Delft rotor

Parameter	Value
Number of blade (N)	2
Rotor diameter (R)	0.6 m
Chord length (c)	0.08 m
Section profile	NACA 0012 airfoil
Blade planform	Rectangular blade

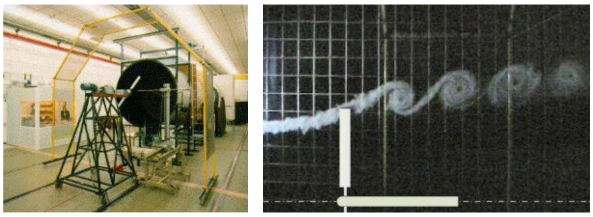

Figure 1. Open jet wind tunnel of DUT and smoke visualization technique (Ref. 13)

The major feature of this measurements is that the range of Reynolds number based on chord length is relatively low all operating conditions because the blade diameter is 0.6m. Hence, it is necessary to take into account the low Reynolds number aerodynamics that cause the nonlinear variation in the lift coefficient with respect to the angle of attack. Experiments provided extensive data on the integrated rotor thrust force and tip vortex trajectories of TU Delft rotor under axial and yawed flow conditions. Therefore, TU Delft rotor model is used to validate the capability of the proposed model, including the prediction of nonlinear aerodynamic loads and wake structures.

TU Delft rotor model is subjected to various with tip speed ratio, tip pitch angle, and yaw angle conditions While the wind speed remains constant during wind tunnel experiment. Flow conditions are listed in Table 2. Aforementioned, the rotor blades are exposed to low Reynolds number flow.

Table 2. Measurements conditions

Parameter	Value
Reynolds number (Re_c)	40,000 ~ 310,000
Wind speed (V)	5.5 m/s
Tip speed ratio (λ)	6, 8, 10
Tip pitch angle (θ_{tip})	0°, 2°, 4°
Yaw angle (β)	0°, ±15°, ±30°, ±45°

Presented at 44th European Rotorcraft Forum, Delft, The Netherlands, 19-20 September, 2018

3.1.2. Axial flow conditions

Numerical prediction of the aerodynamic loads and wake structures of TU Delft rotor model under axial and yawed flow conditions was conducted to validate the accuracy and capability of NVLM and VPM used in this work. The thrust forces which are the force component along normal to the rotating plane, and near wake geometry in terms of the radial and axial positions were available for comparison.

The predicted thrust forces with different tip speed ratio and tip pitch angles were well matched with measurements, as depicted in Figure 2. In wind turbine aerodynamics, increasing tip pitch angle at the same tip speed ratio condition indicates that the local angle of attack decreases and the thrust force eventually decreases. The effects of the tip pitch angle on the aerodynamic performance were similarly observed from numerical simulation and experiments (Refs. 8, 9)

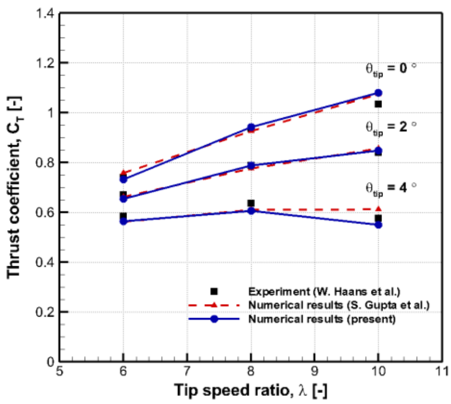

Figure 2. Comparison of the measured and predicted thrust coefficients for axial flow

Figure 3 showed the wind turbine wake structures modelled by vortex particles, and their tip vortex trajectories were compared with the experiments. The comparison results showed that the near wake geometries as a function of axial and radial positions were in good agreement with measured data. It was found that the vortex particle method is capable of accurately modelling the near wake of wind turbine wake. In addition, the helical wake structure can be preserved in the far downstream. At the same tip speed ratio, if the tip pitch angle increases from (a) to (c) in Figure 3, the thrust force decreases owing to the reduction of local angle of attack. It indicates that the momentum reduction in the axial direction decreases, thus leading to decrease in a wake expansion angle and increase in a helical pitch of wake geometry.

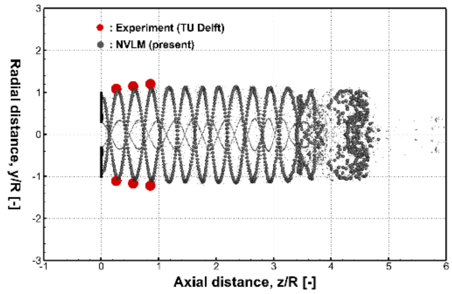

(a) $\lambda = 8$, $\theta_{tip} = 0°$, $\beta = 0°$

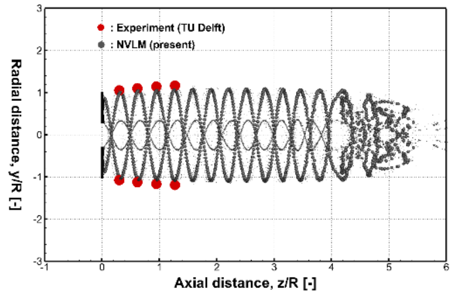

(b) $\lambda = 8$, $\theta_{tip} = 2°$, $\beta = 0°$

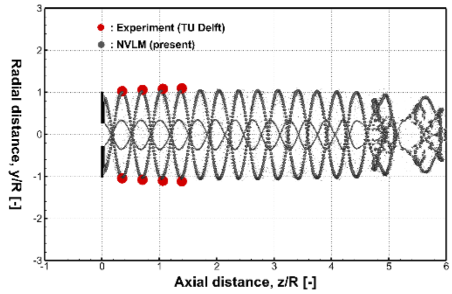

(c) $\lambda = 8$, $\theta_{tip} = 4°$, $\beta = 0°$

Figure 3. Comparison of wind turbine wake structures under axial flow conditions

3.1.3. Yawed flow conditions

When wind turbine is exposed to the yawed flow conditions, the wind turbine wake behind the rotor disc evolves with a deflection angle and the rotor blades experience the azimuthal variation in the aerodynamic loads. NVLM was used to predict the aerodynamic performance and wake dynamics of the yawed-rotor configuration.

Numerical simulation on the TU Delft rotor with various tip pitch and yaw angles at constant tip speed ratio ($\lambda = 8$) was carried out. Figure 4 showed the computed time-averaged thrust forces of TU Delft rotor model in the yawed flow conditions, and compared the results with experimental data (Refs. 8, 9). As illustrated in Figure 4, velocity normal to the rotating plane decreases, while velocity tangential to the rotating plane increases with increasing yaw angles. This eventually results in a decrease in the thrust forces.

Presented at 44th European Rotorcraft Forum, Delft, The Netherlands, 19-20 September, 2018

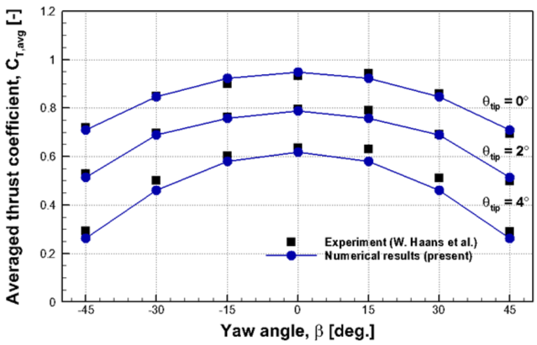

Figure 4. Comparison of the measured and predicted thrust coefficients for yawed flow

Yawed inflow also results in a wake deflection along the yaw direction, as shown in Figure 5. The deflected wake geometries were compared with the measurements with different tip pitch angles. The tip vortex trajectories of near wake in the upwind side matched well with measurements, while those in the downwind side were slightly overestimated. From Figure 5, a strong wake-wake interaction between hub and tip vortices and a strong mixing region in the downstream were captured. The wake vortices shed from the rotor blade in the upwind side became unstable, and began to interact with another vortices as the wake evolves downstream. Finally, the skewed wake structures completely broke down, and merged to form a strong mixing region at the far downstream. From Figure 3 and 5, we observed that VPM used in this work can accurately predict both helical and skewed wake structure and yield a meaningful wake solution.

3.2. NREL Phase VI rotor model

3.2.1. Model description

NREL Phase VI experiment with a dimeter of 10m two-bladed rotor blade was conducted in 24.4m × 36.6m NASA-Ames wind tunnel facility in 2000 (Ref. 21). The measurements have been widely employed to validate the accuracy of aerodynamic models for wind turbine, such as BEM, vortex methods, and CFD. Compared to TU Delft rotor experiments, They provided a variety of measured data, including averaged/time-dependent normal and tangential forces distribution in the spanwise direction, surface pressure distribution, integrated rotor performance at both axial and yawed flow conditions. The rotor blades are comprised of a tapered-twisted configuration without coning, hub tilt, and prebend angles, as listed in Table 3.

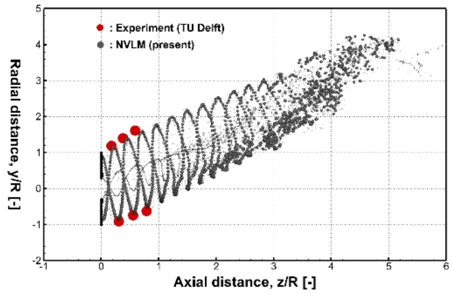

(a) λ = 8, θ_{tip} = 0°, β = 30°

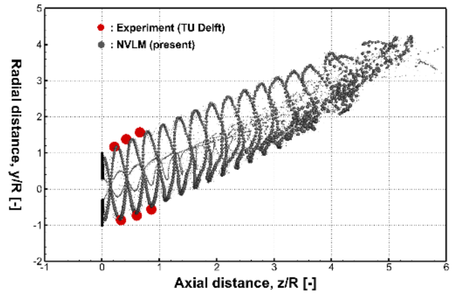

(b) λ = 8, θ_{tip} = 2°, β = 30°

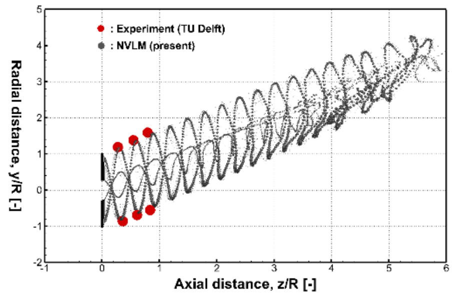

(c) λ = 8, θ_{tip} = 4°, β = 30°

Figure 5. Comparison of tip vortex trajectories under yawed flow conditions

Table 3. Model description of TU Delft rotor

Parameter	Value
Number of blade (N)	2
Rotor diameter (R)	5.029 m
Section profile	S809 airfoil
Blade planform	Tapered-twisted blade

Figure 6. NASA Ames wind tunnel and NREL Phase VI wind turbine configuration (Ref. 15)

Presented at 44th European Rotorcraft Forum, Delft, The Netherlands, 19-20 September, 2018

Table 4. Measurements conditions

Parameter	Value
Wind speed (V)	7 m/s
Tip pitch angle (θ_{tip})	3
Yaw angle (β)	0, 30, 45, 60

3.2.2. Aerodynamic performance

Under yawed flow conditions, the azimuthally varying aerodynamic loads acting on the wind turbine blade were numerically evaluated using the NVLM method and compared with the NREL measurement data (Ref. 21). Wind turbine was subjected to the incoming wind speed of 7 m/s with different yaw angles of 0°, 30°, 45°, and 60°, as listed in Table 4. Comparisons of the averaged normal and tangential forces distribution along radial directions with various yaw angles are shown in Figure 7 and 8. Although NVLM tends to slightly under estimate the averaged normal force at highly yawed conditions, all numerical results for predicting normal an tangential forces generally matched well against experiments. The results showed that the radial distributions of normal and tangential forces computed by NVLM were in quite good agreement with the measured data, even for highly yawed flow conditions.

At yawed-rotor configuration under low wind speed conditions, the skewed wake effect is the dominant factor in determining the azimuthal aerodynamic loads as it directly leads to the variation in the axial induced velocity. Hence, investigating the impact of a non-axisymmetric wake on the unsteady aerodynamic behaviour of the wind turbine blade is needed to accurately predict unsteady blade loading. Figure 9 showed the azimuthal distribution of the axial velocity, the effective angle of attack on the rotor blade, and the thrust force for the axial and yawed flow conditions, respectively. Under axial conditions, the helical wake structure was generated, and was transported toward downstream without the skewness. This leads to the symmetric distribution of the wake-induced velocity and has only radial dependency on the aerodynamic load. On the contrary, both radial and azimuthal dependency on the axial velocity, effective angle of attack, and thrust force were clearly observed under yawed conditions, as depicted in Figure 9. It indicated that the skewed wake structure has a significant role in the unsteady aerodynamic behaviour of the rotor blade and the asymmetric distribution of the wake-induced axial velocity on the rotor blade. Under yawed conditions, the wake was deflected in the direction of the downwind side, and it was unequally expanded, thus leading to a strong expansion downwind of the rotor and a weak expansion upwind of the rotor. Because of the skewed wake geometry, the distance between the trailing tip vortices and rotor plane is closer at the downwind side of the rotor blade compared to the upwind side. The closer the trailing tip vortices are placed on the rotor plane, the lager the magnitude of the induced velocity normal to the rotor plane is induced. Hence, the rotor blade on the downwind side experienced a smaller axial velocity and effective angle of attack than the rotor blade on the upwind side, leading to smaller load. Finally the yawed rotor blades eventually suffered from the aerodynamic loading unbalance between the upwind and downwind sides of the rotor plane. For the outboard region, this consequently yields a restoring moment, referred to as a stabilizing moment. The yaw aerodynamics associated with a skewed wake effect were confirmed in literature (Refs. 9, 15)

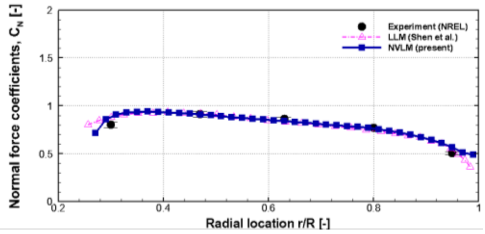

(a) Yaw angle, β = 0 °

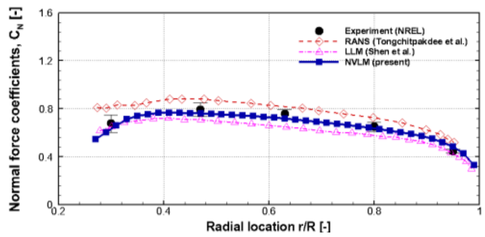

(b) Yaw angle, β = 30 °

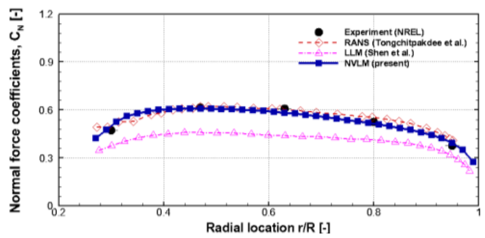

(c) Yaw angle, β = 45 °

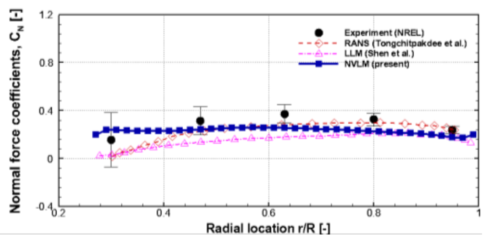

(d) Yaw angle, β = 60 °

Figure 7. Comparison of the averaged normal force coefficient depending on yaw angles

Presented at 44th European Rotorcraft Forum, Delft, The Netherlands, 19-20 September, 2018

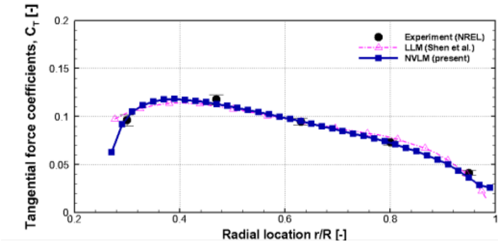

(a) Yaw angle, β = 0 °

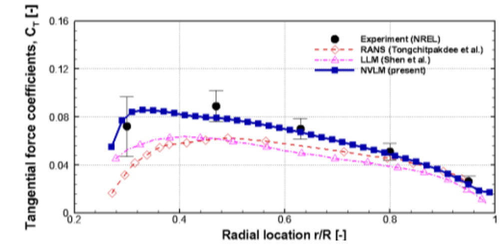

(b) Yaw angle, β = 30 °

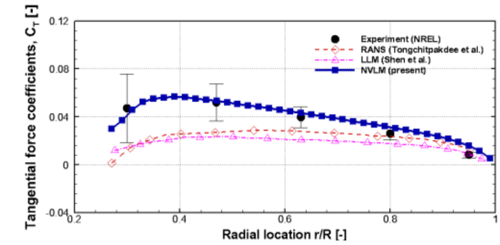

(c) Yaw angle, β = 45 °

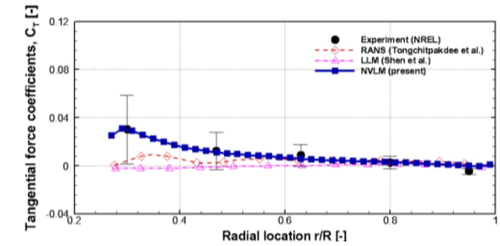

(d) Yaw angle, β = 60 °

Figure 8. Comparison of the averaged tangential force coefficient depending on yaw angles

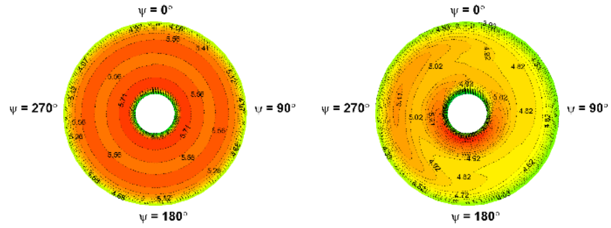

(a) Effective axial velocity

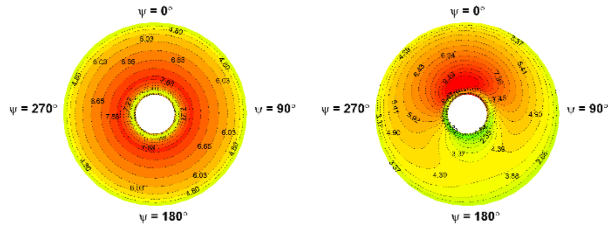

(b) Effective angle of attack

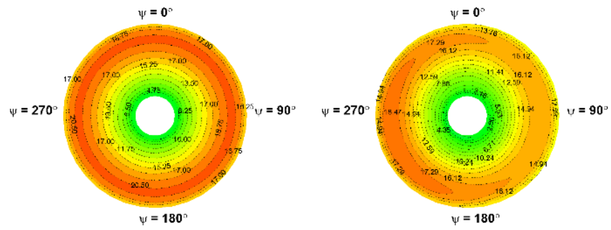

(c) Thrust force

Figure 9. Contours of effective axial velocity, effective angle of attack, and thrust force at β = 0° (left) and 30° (right)

3.2.3. Vorticity fields in the downstream

Figure 10 showed the vorticity contours in the z-direction at the different downstream locations where the contour planes (XY planes) are placed at z/R = 4, 6, 8, 10 and 12 downstream. An approximately symmetrical and circular vorticity fields around the rotor area can be clearly observed at axial flow condition. On the contrary, the asymmetric vorticity fields were developed as a result of the skewed wake geometry at yawed conditions. The curled vorticity field arising from the yawed-rotor configuration yielded a highly complex flow field with large gradients. It is much more pronounced as the wake propagated toward downstream. It can significantly affect the inflow condition and the rotor aerodynamic performance of the subsequent wind turbines in a particular wind farm array. Therefore, it should be taken into account in order to evaluate an overall power output of a wind farm and to design the optimal array of wind turbines.

Presented at 44th European Rotorcraft Forum, Delft, The Netherlands, 19-20 September, 2018

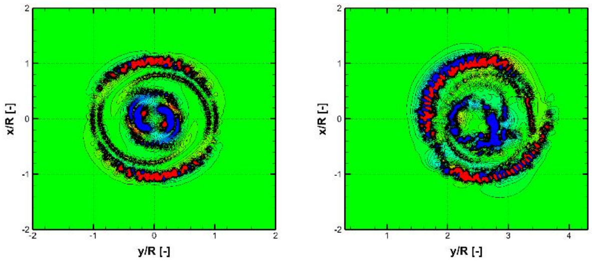

(a) Vorticity contours at z/R = 4

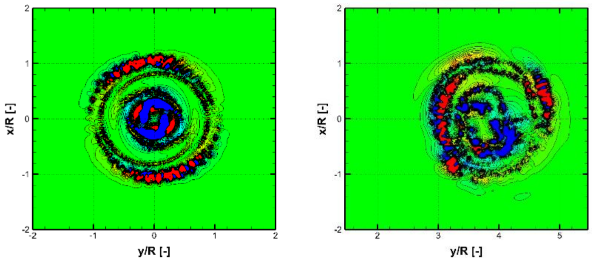

(b) Vorticity contours at z/R = 6

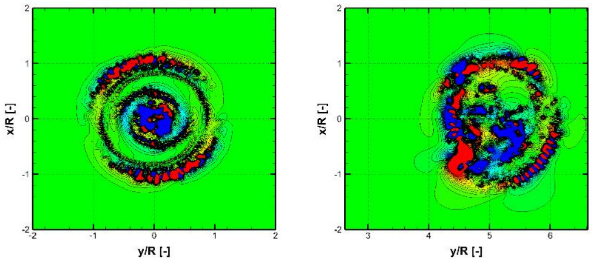

(c) Vorticity contours at z/R = 8

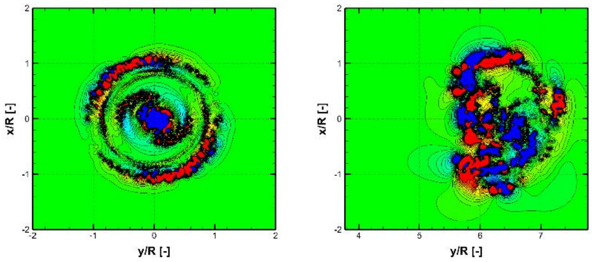

(d) Vorticity contours at z/R = 10

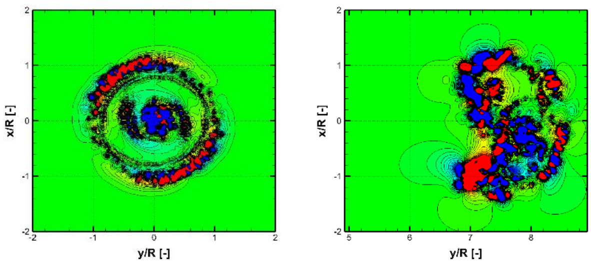

(e) Vorticity contours at z/R = 12

Figure 10. Vorticity contours in the wake region depending on downstream positions at β = 0° (left) and 30° (right)

4. CONCLUSION

To study the yaw aerodynamics and the impacts of the skewed wake structure on the blade loading, the numerical simulation of the TU Delft and NREL Phase VI wind turbine models exposed to yawed flow was carried out, and these results were compared against the experiments. The comparison results showed that NVLM predictions for the aerodynamic loads matched well with the measurements, even for highly yawed conditions. In addition, the effects of skewed wake geometry and wake behaviours were discussed in detail to achieve a better understanding of the skewed wake characteristics. Under the axial flow, helical wake and symmetric vorticity fields developed downstream. Their structures can be preserved and transported along the rotating axis in the far wake field. On the contrary, wake was deflected toward the downwind side of the rotor blade and an asymmetrically curled vorticity field around the rotor area was clearly observed in the yawed-rotor configuration. The skewed wake structure became highly unstable, and it completely broke down as the wake propagated downstream.

The necessity of an in-depth understanding of yaw aerodynamics and skewed wake has recently been recognized as intentional yaw misalignment in the upstream wind turbine can alleviate the power loss of downstream wind turbines in the wind farm. This provides a scope for further research to predict the overall power output and analyse the unsteady wake dynamics of a wind farm where a great number of wind turbines will be installed in close proximity to each other.

5. REFERENCE

[1] Ryu, K.W., Kang, S.H., Seo, Y.H., and Lee, W.R., "Prediction of Aerodynamic Loads for NREL Phase VI Wind Turbine Blade in Yawed Condition," International Journal of Aeronautical and Space Sciences, 17(2), 2016, pp. 157-166.

[2] Duque, E.P.N., Burklund, M.D., and Johnson, W., "Navier-Stokes and Comprehensive Analysis Performance Predictions of the NREL Phase VI Experiment," Journal of Solar Energy Engineering, 125(4), 2003, pp. 457-467.

[3] Shen, X., Zhu, X., and Du, Z., "Wind turbine aerodynamics and loads control in wind shear flow," Energy, 36, 2011, pp. 1424-1434.

[4] Tongchitpakdee, C., Benjanirat, S., and Sankar, L.N., "Numerical Simulation of the Aerodynamics of Horizontal Axis Wind Turbines under Yawed Flow Conditions," Journal of Solar

Energy Engineering, 127(4), 2005, pp. 464-474.

[5] Yu, D.O., You, J.Y., and Kwon, O.J., “Numerical investigation of unsteady aerodynamics of a Horizontal-axis wind turbine under yawed flow conditions,” Wind Energy, 16, 2013, pp.711-727.

[6] Vermeer, L.J., “A Review of Wind Turbine Wake Research at TU Delft,” 20th ASME Wind Energy Symposium, 39th Aerospace Sciences Meeting and Exhibit, AIAA-2001-0030, 2001.

[7] Vermeer, L. J., Sørensen, J. N., and Crespo, A., “Wind Turbine Wake Aerodynamics,” Progress in Aerospace Sciences, Vol. 39, 2003, pp.467-510.

[8] Haans, W., Sant, T., van Kuit, G., and van Bussel, G., “Measurement and Modelling of Tip Vortex Paths in the Wake of a HAWT under Yawed Flow Conditions,” AIAA 2005-590, 43rd AIAA Aerospace Sciences Meeting and Exhibit, Reno, Nevada, 2005

[9] Haans, W., Sant, T., van Kuik, G., and van Bussel, G., “Measurement of Tip Vortex Paths in the Wake of a HAWT Under Yawed Flow Conditions,” Journal of Solar Energy Engineering, 127(4), 2005, pp. 456-463.

[10] Grant, I., Parkin, P., and Wang, X., “Optical vortex tracking studies of a horizontal axis wind turbine in yaw using laser-sheet, flow visualisation,” Experiments in Fluids, 23(6), 1997, pp. 513-519.

[11] Grant, I. and Parkin, P., “A DPIV study of the trailing vortex elements from the blades of a horizontal axis wind turbine in yaw,” Experiments in Fluids, 28(4), 2000, pp. 368-376.

[12] Bastankhah, M, and Porté-Agel, F., “A wind-tunnel investigation of wind-turbine wakes in yawed conditions,” Journal of Physics: Conference Series, 625, 2015, pp. 012014.

[13] Bartl, J. and Sætran, L. “Blind test comparison of the performance and wake flow between two in-line wind turbines exposed to different turbulent inflow conditions,” Wind Energy Science, 2, 2017, pp. 55-76.

[14] Howland, M.F., Bossuyt, J., Martínez-Tossas, L.A., Meyers, J., and Meneveau, C., “Wake structure in actuator disk models of wind turbines in yaw under uniform inflow condition,” Journal of Renewable and Sustainable Energy, 8, 2016, pp. 043301.

[15] Lee, H.J., Jo, Y.M., and Lee, D.J., “Development of Nonlinear Vortex Lattice Method and Its Application to Aerodynamic Analysis of Wind Turbine,” 6th Asian/Austrailian Rotorcraft Forum and Heli Japan, 2017.

[16] Jo, Y.M., Lee, H.J., and Lee, D.J., “Prediction of Rotor Flow for Unmanned Aerial System Using Nonlinear Vortex Lattice Method,” 6th Asian/Australian Rotorcraft Forum and Heli Japan, 2017.

[17] Lee, D. J. and Na, S. U., “Numerical Simulations of Wake Structure Generated by Rotating Blades using a Time Marching, Free Vortex Blob Method,” European Journal of Mechanics – B/Fluids, Vol. 18 (1), 1999, pp.147-159.

[18] Winckelmans, G. S., “Topics in Vortex Methods for the Computation of Three- and Two-Dimensional Incompressible Fluid,” Ph. D. dissertation, California Institute of Technology, 1989.

[19] Park, S. H., Chu, Y. B., and Lee, D. J., “Investigation of Main Rotor-Tail Rotor Interaction in Hover Flight using Vortex Particle Method,” 5th Asian-Australian Rotorcraft Forum, Singapore, November 17-18, 2016.

[20] Park, S. H., Chu, Y. B., Lee, D. J., and Jang, J. S., “Trimmed Simulation of a Complete Helicopter Configuration in Hover Flight,” AHS 72nd Annual Forum, West Palm Beach, Florida, USA, May 17-19, 2016.

[21] Hand, M. M., Simms, D. A., Fingersh, L. J., Jager, D. W., Cotrell, J. R., Schreck, S. and Larwood, S. M., “Unsteady Aerodynamics Experiment Phase VI: Wind Tunnel Test Configurations and Available Data Campaigns,” Technical Report, NREL/TP-500-29955, 2001

Presented at 44th European Rotorcraft Forum, Delft, The Netherlands, 19-20 September, 2018